FEBS Letters 399 (1996) 166–170 FEBS 17837

The oligomerization domain of p53: Crystal structure of the trigonal form

Maria Miller[a,*], Jacek Lubkowski[a], J.K. Mohana Rao[a], Avis T. Danishefsky[a,b], James G. Omichinski[c], Kazuyasu Sakaguchi[d], Hiroshi Sakamoto[d], Ettore Appella[d], Angela M. Gronenborn[c], G. Marius Clore[c]

[a]*Macromolecular Structure Laboratory, NCI-Frederick Cancer Research and Development Center, ABL-Basic Research Program, Frederick, MD 21702, USA*
[b]*Department of Medical Research and Technology, University of Maryland at Baltimore, Baltimore, MD 21201-1082, USA*
[c]*Laboratory of Chemical Physics, Building 5, National Institute of Diabetes and Digestive and Kidney Diseases, National Institutes of Health, Bethesda, MD 20842, USA*
[d]*Laboratory of Cell Biology, Building 37, National Cancer Institute, National Institutes of Health, Bethesda, MD 20842, USA*

Received 25 June 1996; revised version received 15 October 1996

Abstract The structure of the oligomerization domain of the p53 tumor suppressor protein was determined in the trigonal crystal form, using a refined NMR structure as a model. A synthetic peptide comprising residues 319–360 of human p53 crystallized in the space group $P3_121$. There is one biologically relevant tetrameric domain in the crystallographic asymmetric unit. The structure was refined jointly with NMR data, only the third such case (the previous examples being IL-1β (Shaanan, B., Gronenborn, A.M., Cohen, G.H., Gilliland, G.L., Veerapandian, B., Davies, D.R. and Clore, G.M. (1992) Science 257, 961–964 [1]) and BPTI (Schiffer, C., Huber, R., Wuthrich, K. and Van Gunsteren, W.F. (1994) J. Mol. Biol. 241, 588–599 [2])), to 2.5 Å resolution with an *R* factor of 0.207. The distribution of tumor-derived mutations in the oligomerization region together with structural and biological data suggest a strategy for the design of antitumor therapeutics.

Key words: p53; Tumor suppressor; Tetramerization domain; X-ray crystallography; NMR; Joint refinement

1. Introduction

The DNA-binding phosphoprotein, p53 functions as a tumor suppressor in human cells by activating transcription of genes that mediate cell cycle arrest and DNA damage repair [3–5] and by inducing apoptosis in response to the activation of oncogenes [6,7]. In this way, p53 controls cell proliferation, and indeed 50% of human cancers have been shown to be associated with mutations in p53. Wild-type (w-t) p53 is active as tetramer and its biological function depends on its ability to self-associate, as well as on interactions with other cellular and viral proteins. The p53 protein comprises a transactivating region, a DNA-binding region, and an oligomerization region [8–10]. The C-terminal region also shows non-specific binding to single-stranded DNA and RNA and enhances specific DNA binding by the whole molecule [11]. Although the oligomerization is necessary for tumor suppressor activity, the tetramerization domain is responsible for the negative dominant mechanism since p53 molecules with mutations in the DNA-binding region can form heterotetramers with w-t p53 via the oligomerization domain, thus sequestering the w-t protein into non-functional tetramers [12]. For these reasons, the structural mechanism of oligomerization is of great interest.

The structure of the oligomerization domain has been determined by NMR [13–16] and by X-ray crystallography [17] methods using slightly different peptide segments. Discrepancies between the crystal structure [17] and the initial NMR structures [13,14] of this protein point out the technical difficulties involved in solving the solution structure of this symmetric homotetramer [15]. Two NMR structures [14,16] show significant (up to 20°) differences in interhelical angles. Although the refined NMR structure [15,16] agrees remarkably well with the crystal structure [17], the latter is a tetramer with a perfect crystallographic 222 symmetry.

Here we describe the crystal structure of the p53 tetramerization domain, in a trigonal crystal form, with the entire tetramer in the crystallographic asymmetric unit. Unambiguous solution was obtained using NMR tetramer [16] as a probe for molecular replacement, and the final refinement was performed jointly against experimental data from crystal and solution studies. Thus, the results obtained confirm that the structure of p53 tetramerization domain is unique and stable, independently of environmental features. On the other hand, observed differences in the conformations of several residues located on the surface of the tetramer allow a re-evaluation of their importance to the stability of the tetramer.

2. Materials and methods

The peptide corresponding to residues 319–360 of human p53 was obtained by chemical synthesis. Crystals grew as rhombohedral plates at room temperature, using the hanging-drop or sitting-drop vapor diffusion method and 55–65% saturated ammonium phosphate solutions. Crystals belonged to the trigonal space group $P3_121$, $a = 51.0$ Å and $c = 113.3$ Å, with one tetramer in the asymmetric unit. Diffraction extended up to 2.0 Å, but the intensity fell off rapidly below 3 Å. Data were collected from a single crystal to 2.1 Å nominal resolution, using the RAXIS IIC imaging plate and were processed with the Molecular Structure Corp. software. A total of 16849 accepted observations ($I \geq 1.0\ \sigma_I$) were reduced to 7387 unique reflections out of 10975 possible to 2.1 Å resolution; the R_{symm} was 0.081. The completeness of the data was 82% to 2.7 Å resolution ($R_{symm} = 0.071$) and 71% to 2.5 Å ($R_{symm} = 0.076$). In each 0.1 Å shell between the 2.6 and 2.2 Å resolution range the data were only 50% complete and the mean I/σ_I was 1.7.

The structure was solved by molecular replacement [18], using the

*Corresponding author. Fax: (1) (301) 846-7101.

Published by Elsevier Science B.V.
PII S0014-5793(96)01231-8

refined mean coordinates of the NMR tetramer [16] as the probe. All atoms from residues 325–355 were used in the model. Rotation and translation searches, as well as the subsequent refinement cycles, were performed using the X-PLOR (version 3.1) package [19]. As expected, the rotation search gave four peaks related by non-crystallographic symmetry (NCS). At 10–4 Å resolution, these peaks were higher than the fifth peak by one standard deviation. A translation search in $P3_121$ gave an unambiguous peak with an R factor of 0.489 in the 10–3.5 Å resolution range, whereas a translation search in the enantiomeric space group $P3_221$ did not result in any significant peak.

For the crystallographic refinement 8% of reflections were removed from the 8–2.7 Å resolution range for the R_{free} calculations [20]. Rigid body refinement of the four monomers decreased the R factor to 0.445 (R_{free} 0.467). An inspection of the crystal packing in the original molecular replacement solution revealed several close contacts involving side chains of symmetry-related molecules. Initially, the side chains of Arg-335 and Arg-342 were replaced with Ala in each subunit. Even then the refinement with strictly constrained NCS resulted in either high R values or the loss of secondary structure elements. Therefore, tightly restrained NCS was applied instead. After the first simulated annealing and positional refinement in the 8–2.7 Å resolution range (using effective force constants for NCS restraints of 400 and 200 kcal mol^{-1} Å^{-2} for the main chain and side chains, respectively), the R factor decreased to 0.355 (R_{free} 0.413). All missing Arg side-chains were modeled back and the refinement was continued with NCS restraints of 250 kcal mol^{-1} Å^{-2} for all residues, except those involved in the crystal contacts. After extensive rebuilding with program FRODO [21] followed by simulated annealing and positional refinement, the structure was refined to an R factor of 0.239 (R_{free} 0.317).

This model was then subjected to joint X-ray and NMR refinement [1] against all unique reflections in the 8–2.5 Å resolution range and 4084 experimental NMR restraints (see Table 1). (Note, as the tetramer is completely symmetric in solution, the latter corresponds to 1021 independent observables.) Refinements were performed using the program X-PLOR with a simulated annealing protocol [22], incorporating coupling constant [23] and carbon chemical shift [24] restraints in addition to the usual X-ray structure factor restraints and NMR-derived interproton distance and torsion angle restraints. The weights for NMR restraints and the crystallographic pseudo-energy term (w_a) were chosen by trial and error. After each round of manual intervention and refinement, the quality of the model was tested by the program PROCHECK [25] and the refinement parameters were adjusted until satisfactory geometry and agreement with electron density were achieved. Residues 319–324 and 356–360, corresponding to the N- and C-termini of the peptide used for crystallization, could not be traced in the electron density for all monomers. These residues were highly mobile in solution structure [16], and only segments 325–365 were traced in the tetragonal crystal form [17]. The peaks in (F_o-F_c) difference Fourier maps within 3.6 Å from the protein atoms were interpreted as water molecules. Only those involved in hydrogen-bond interactions and with B values smaller then 60 Å^2 after refinement were retained. Refinement of individual temperature factors (B_{iso}), with NCS restraints set to 25 kcal mol^{-1} Å^{-2}, resulted in an R factor of 0.207 with good geometry and an average B_{iso} of 29.5 Å^2 for protein atoms.

Simulated annealing under the same conditions with 8% of reflections excluded from the refinement resulted in a model of unchanged quality with an R factor of 0.205 (R_{free} 0.296). When NMR restraints were removed from the refinement, while w_a was unchanged, the values were 0.200 and 0.301 for R factor and R_{free}, respectively, but the quality of the model was worse (see Table 1). The high content of disordered residues in the crystal probably accounts for the poor diffraction by the crystal and the high R_{free}/R factor ratio of the refined models.

3. Results and discussion

The model of the human p53 tetramerization domain (Fig. 1) consists of four crystallographically independent subunits, designated A–D as in the NMR model [16], and 80 water molecules. The electron density corresponding to monomers B and D is very well defined. Several residues of monomer A and C, either strained by crystal contacts or exposed to solvent channels, are partially disordered. The homotetramer has

Table 1
Structural statistics[a]

Structural statistics	Final model X-ray/NMR	SA refinement of the final model	
		X-ray/NMR	X-ray
X-ray restraints			
R factor (4722/4338)[b]	0.207	0.205	0.200
R_{free} (384)	–	0.297	0.301
NMR-derived restraints (4084)[c]			
rmsd from:			
NOE-derived distance restraints (Å) (3520)[c]	0.075 [14]	0.077 [19]	0.173 [86]
Dihedral angle restraints (°) (224)[c]	3.25 [22]	2.79 [19]	10.91 [41]
$^3J_{HN\alpha}$ coupling constants (Hz) (112)[c]	1.49 [48]	1.47 [48]	1.74 [60]
Chemical shifts (ppm)			
$^{13}C_\alpha$ (116)	0.74	0.71	0.80
$^{13}C_\beta$ (112)	1.13	1.14	1.21
Deviations from idealized covalent geometry			
Bonds (Å) (2260)	0.011	0.011	0.011
Angles (°) (3836)	1.26	1.27	1.23
Impropers (°) (1128)	3.10	3.09	3.09
% residues in the most favoured Ramachandran plot areas	95.5	93.8	88.4
Bad contacts/100 residues	18	23	30

[a]The number of terms for the complete tetramer for various restraints is given in parentheses.
[b]The first number indicates the total number of reflections (8–2.5 Å resolution range) used for the final refinement; the second number indicates that used for the R_{free} refinement.
[c]The total number of independent experimental NMR restraints is 1021 due to the symmetric nature of the tetramer. The force constants for the various terms in the target function are as follows: 15 kcal mol^{-1} Å^{-2} and 100 kcal mol^{-1} rad^{-2} for the square-well interproton distance and torsion angle restraints terms, respectively; 0.5 kcal mol^{-1} Hz^{-2}, 0.5 kcal mol^{-1} ppm^{-2}, 25 kcal mol^{-1} Å^{-2}, 1000 kcal mol^{-1} Å^{-2}, 500 kcal mol^{-1} rad^{-2}, and 500 kcal mol^{-1} rad^{-2} for the harmonic coupling constant, chemical shift, NCS, bond, angle, and improper torsion terms, respectively; 4 kcal mol^{-1} Å^{-4} for the quartic van der Waals repulsion term, with the hard sphere van der Waals radii set to 0.8 times the standard van der Waals radii used in the PARAM19/PARAM20 CHARMM parameters; $w_a = 1.25 \times 10^5$. The number of violations of interproton distance, torsion angle, and $^3J_{HN\alpha}$ coupling constant greater than 0.5 Å, 5°, and 1 Hz, respectively, is indicated in square brackets.


N(B)
N(C)
N(D)
N(A)


R542
E546

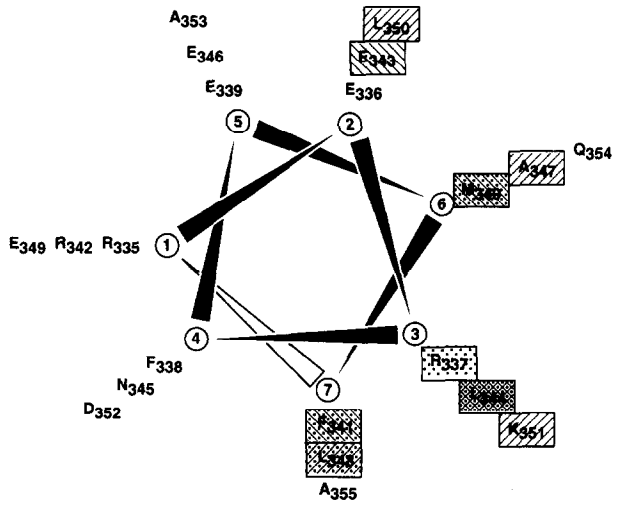

Fig. 2. Helical wheel representation of an α-helix formed by residues 335–353 of human p53. Residues involved in the helix-helix hydrophobic interactions between subunits of the tetramerization domain are boxed. Residues involved in the interactions between monomers AC, AB, or AD are marked by :::, ///, or \\\, respectively.

approximate 222 symmetry with deviations of 1.0, 1.9, and 0.4° from the ideal 2-fold relating subunits A and B, A and C, and A and D, respectively. Corresponding rmsd values are 0.47, 0.42, and 0.52 Å for the superposition of C_α atoms; however, these values are less than 0.3 Å for the superposition of all the atoms from residues not involved in the crystal contacts. This slight asymmetry is caused by the crystal packing and does not affect intersubunit interfaces (see also [16]). While inclusion of the NMR observations in the refinement had negligible effect on the appearance of electron density, the resulting model has improved stereochemistry and is compatible with data from crystal and solution studies.

Each subunit of the homotetramer comprises a β-strand (residues 326–333) and a tight turn (Gly-334), followed by an α-helix (residues 335–353). The hairpin structure of the monomer is maintained by hydrophobic clusters formed by Leu-330, Ile-332, Phe-338, and Phe-341 and is further stabilized by the hydrogen bond formed by the guanidinium group of Arg-337 and the main-chain carbonyl oxygen of Arg-333.

The topology of the tetramer may best be described as a dimer of dimers, with the two dimers arranged orthogonally to each other (see Fig. 1). Each primary dimer (subunits AC and BD) consists of two antiparallel α-helices and an antiparallel two-stranded β-sheet. The interface between the two dimers is formed by the interactions of their α-helices, which form a four-helix bundle. The β-sheets are located on the opposite side of the tetramer.

Residues involved in the hydrophobic helix-helix contacts are located at positions 2, 3, 6, and 7 of the helical wheel representation shown in Fig. 2. Leu-344 (located close to the center of the tetramer) seems to be crucial for tetramer formation, since this residue is involved in the interhelical interactions between monomers AC, AB, and AD. Mutation of Leu-344 to Ala results in the binding of p53 to DNA as a dimer [26]. Phe-338 and Phe-341 interact with the hydrophobic side of the β-sheets located outside the helix bundle, providing additional stabilization of the AC interface. The primary dimer is also stabilized by a salt bridge between the carboxylate of Asp-352A and the guanidinium group of the partially buried Arg-337C.

Residues Arg-335, Arg-342, Glu-349, Glu-339, Glu-346, and Ala-353, located at positions 1 and 5 of the helical wheel (Fig. 2), are exposed to solvent. As shown in Fig. 3, two tetramers in the crystal are related by crystallographic symmetry and are held together by the interactions of their antiparallel aligned helices, with Arg-342 and Glu-346 forming salt bridges with symmetry-related Glu-346 (#Glu-346) and #Arg-342, respectively. These interactions suggest a possible mode for additional oligomerization of p53, which has been observed in vitro [27]. In vivo, the exposed polar side of each helix of the tetramerization domain presents a possible site of p53 interactions with other cellular or viral proteins, reported to form complexes with p53 [28]. This possibility is supported by the finding [29] that the mutation of Glu-349 to Asp occurs in a number of human tumors. Glu-349 is involved in crystal contacts and does not seem to contribute to the stability of the tetramerization domain. Glu-349 is probably important for either interdomain or intermolecular interactions. On the other hand, three other mutations found in human tumors within the ordered part of the oligomerization domain (i.e., substitution of His for Leu-330, Val for Gly-334, and Cys for Arg-337) involve residues that, as described above, are critical for maintaining the structure of the monomer and are also important for stabilizing the primary dimer.

The overall structure agrees very well with published crystallographic [17] and solution [16] models. The rmsd values for the C_α atoms of residues 325–355 when the entire tetrameric model was superimposed on the NMR structure [16] or the tetragonal crystal structure [17] were 0.73 and 0.48 Å, respectively. The differences in conformations are observed only for residues located on the surface of the tetramer. Water molecules identified in the NMR structure [16] are well defined in the electron density near the main-chain amide groups of Arg-333 in monomers A and B. The conformation of Tyr-327 in each monomer is different from that in reported structures [16,17] and, therefore, intermonomer hydrogen bond formation with Arg-333 as described for the tetragonal form of crystal structure [17] is not possible. Also, a hydrogen bond involving Lys-351A and the main-chain carbonyl oxygen of Glu-343B [16] is not observed. Thus, the interface between the two primary dimers is entirely hydrophobic and should be potentially disruptable by small molecule compounds.

The fact that none of the residues from this interface have been found mutated in tumors supports the hypothesis that the function of the w-t allele is abrogated in a dominant negative fashion by formation of inactive heterotetramers composed of w-t and mutated p53 monomers. This effect may be significantly reduced by inhibitors of tetramerization.

←
Fig. 1. (Above) Tetramerization domain of p53 protein. Subunits A, B, C, and D are colored red, green, yellow, and purple, respectively.

←
Fig. 3. (Below) Crystal contacts formed by two tetramers in the trigonal crystal lattice.

The biological data [4,8] and the location of tumor-derived mutations (vide supra) indicate that inducing the dissociation to monomers would result in the loss of p53 tumor suppressor activity. Therefore, effective drugs should selectively prevent the association of the two principal dimers, since the transactivating function of p53 is retained by its dimeric form [4]. In cells expressing one w-t p53 allele such an approach may generate a sufficient number of w-t homodimers to partially restore p53 function.

Acknowledgements: We thank Dr. Alexander Zdanov for help with the X-ray data processing and Dr. Peter F. Johnson for critical reading of the manuscript. This research is sponsored in part by the National Cancer Institute, DHHS, under contract with ABL and by the Intramural AIDS Targeted Antiviral Program of the Office of the NIH Director (G.M.C., A.M.G. and E.A.). The contents of this publication do not necessarily reflect the views or policies of the Department of Health and Human Services, nor does mention of trade names, commercial products, or organizations imply endorsement by the U.S. Government.

References

[1] Shaanan, B., Gronenborn, A.M., Cohen, G.H., Gilliland, G.L., Veerapandian, B., Davies, D.R. and Clore, G.M. (1992) Science 257, 961–964.
[2] Schiffer, C., Huber, R., Wuthrich, K. and Van Gunsteren, W.F. (1994) J. Mol. Biol. 241, 588–599.
[3] Fields, S. and Jang, S.K. (1990) Science 249, 1046–1049.
[4] Pietenpol, J.A., Tokino, T., Thiagalingam, S., El-Deiry, W.S., Kinzler, K.W. and Vogelstein, B. (1994) Proc. Natl. Acad. Sci. USA 91, 1998–2002.
[5] Harper, J.W., Adami, G.R., Wei, N., Keyomarsi, K. and Elledge, S.J. (1993) Cell 75, 805–816.
[6] Hermeking, H. and Eick, D. (1994) Science 265, 2091–2093.
[7] Wu, X. and Levine, A.J. (1994) Proc. Natl. Acad. Sci. USA 91, 3602–3606.
[8] Stenger, J.E., Tegtmeyer, P., Mayr, G.A., Reed, M., Wang, Y., Wang, P., Hough, P.V. and Mastrangelo, I.A. (1994) EMBO J. 13, 6011–6020.
[9] Friedman, P.N., Chen, X., Bargonetti, J. and Prives, C. (1993) Proc. Natl. Acad. Sci. USA 90, 3319–3323.
[10] Sakamoto, H., Lewis, M.S., Kodama, H., Appella, E. and Sakaguchi, K. (1994) Proc. Natl. Acad. Sci. USA 91, 8974–8978.
[11] Jayaraman, J. and Prives, C. (1995) Cell 81, 1021–1029.
[12] Shaulian, E., Zauberman, A., Ginsberg, D. and Oren, M. (1992) Mol. Cell. Biol. 12, 5581–5592.
[13] Clore, G.M., Omichinski, J.G., Sakaguchi, K., Zambrano, N., Sakamoto, H., Appella, E. and Gronenborn, A.M. (1994) Science 265, 386–391.
[14] Lee, W., Harvey, T.S., Yin, Y., Yau, P., Litchfield, D. and Arrowsmith, C.H. (1994) Nat. Struct. Biol. 1, 877–890.
[15] Clore, G.M., Omichinski, J.G., Sakaguchi, K., Zambrano, N., Sakamoto, H., Appella, E. and Gronenborn, A.M. (1995) Science 267, 1515–1516.
[16] Clore, G.M., Ernst, J., Clubb, R., Omichinski, J.G., Kennedy, W.M., Sakaguchi, K., Appella, E. and Gronenborn, A.M. (1995) Nat. Struct. Biol. 2, 321–333.
[17] Jeffrey, P.D., Gorina, S. and Pavletich, N.P. (1995) Science 267, 1498–1502.
[18] Rossmann, M.G. (1972) The Molecular Replacement Method, a Collection of Papers on the Use of Non-crystallographic Symmetry, Gordon and Breach, New York.
[19] Brunger, A. (1992) X-PLOR Version 3.1: A System for X-Ray Crystallography and NMR, Yale University Press, New Haven, CT.
[20] Brunger, A.T. (1992) Nature 355, 472–474.
[21] Jones, T.A. (1978) J. Appl. Crystallogr. 11, 268–272.
[22] Nilges, M., Clore, G.M. and Gronenborn, A.M. (1988) FEBS Lett. 229, 317–324.
[23] Garrett, D.S., Kuszewski, J., Hancock, T.J., Lodi, P.J., Vuister, G.W., Gronenborn, A.M. and Clore, G.M. (1994) J. Magn. Reson. B. 104, 99–103.
[24] Kuszewski, J., Qin, J., Gronenborn, A.M. and Clore, G.M. (1995) J. Magn. Reson. B. 106, 92–96.
[25] Laskowski, R.A., MacArthur, M.W., Smith, D.K., Jones, D.T., Hutchinson, E.G., Morris, A.L., Naylor, D., Moss, D.S. and Thornton, J.M. (1994) PROCHECK v.3.0, University College, London.
[26] Waterman, J.L., Shenk, J.L. and Halazonetis, T.D. (1995) EMBO J. 14, 512–519.
[27] Kraiss, S., Quaiser, A., Oren, M. and Montenarh, M. (1988) J. Virol. 62, 4737–4744.
[28] Pietenpol, J.A. and Vogelstein, B. (1993) Nature 365, 17–18.
[29] Cariello, N.F., Cui, L., Beroud, C. and Soussi, T. (1994) Cancer Res. 54, 4454–4460.